Int. J. Electrochem. Sci., 8 **(2013)** 11215 - 11227

International Journal of ELECTROCHEMICAL SCIENCE
www.electrochemsci.org

A Biosensor for Detect Nitrite (NO_2^-) and Hydroxylamine (NH_2OH) by Using of Hydroxylamine Oxidase and Modified Electrode with ZnO Nanoparticles

Masoud Mohammadian[1], Ladan Farzampanah[2], Afsaneh Behtash-oskouie[3], Sahar Majdi[4], Gholamreza Mohseni[5], Mojtaba Imandar[6], Maryam Shirzad[2], Reza Soleimani[2], Masoud Negahdary[7,]*

[1] Department of Microbiology, Zanjan University of Medical Sciences, Zanjan, Iran
[2] Department of Biology, Payame Noor University, I.R. of IRAN
[3] Department of Chemical Engineering, Shahre-Rey Branch Branch, Islamic Azad University, Shahre-Rey, Iran
[4] Department of Biochemistry, Science and Research Branch, Islamic Azad University, Tehran, Iran
[5] Department of Anesthetics, Shahid Beheshti University of Medical Sciences, Tehran, Iran
[6] Dept. of Agriculture, Payame Noor University, POB 19395-4697, I.R. of Iran
[7] Yazd Cardiovascular Research Center, Shahid Sadoughi University of Medical Sciences, Yazd, Iran
[*]E-mail: Masoud.negahdary@hotmail.com

Received: 17 May 2013 / *Accepted:* 15 July 2013 / *Published:* 20 August 2013

The direct electrochemistry of Hydroxylamine oxidase (HAO) / zinc oxide (Zno) nanoparticles (Nps) /carbon paste electrode (CPE) was studied for design a new biosensor for detect Nitrite (NO_2^-) and hydroxylamine (NH_2OH). A conventional three electrode cell was employed throughout the experiments, with bare or Zno nanoparticles/ HAO modified carbon paste electrode (4.0 mm diameter) as a working electrode, an Ag/AgCl as a reference electrode and a platinum electrode as a counter electrode; all electrochemical study done by voltammetric method (here cyclic voltammetry (CV)). Samples were measured and recorded using a TU-1901 double-beam UV-visible (UV-VIS) spectrophotometer and phase characterization was performed by means of X-ray diffraction (XRD) and also the morphologies and particle sizes of the samples were characterized by scanning electron microscopy (SEM). The results showed that the redox process was an adsorption-controlled and the immobilized Hydroxylamine oxidase was stable and could detect NO_2^- concentration in solution in the range of 5 to 43 μM; also mentioned biosensor could detect hydroxylamine at surface of modified CPE with Zno (Nps).

Keywords: biosensor, Nitrite, hydroxylamine, Hydroxylamine oxidase, ZnO Nanoparticles

1. INTRODUCTION

The Hydroxylamine oxidase (HAO) enzyme that is a homotrimer which binds a remarkable total of 24 haem groups, aligned to form a ring that has inlet and outlet sites. Each monomer binds eight haems; seven c-type haems, and a novel haem designated P460 which has a tyrosine residue attached to the tetrapyrrole ring [1-3]. The c-type haem irons are all coordinated by two histidine residues, while that of P460 is coordinated by one, with the extra site on the iron being available for substrate binding [4]. The oxidation of hydroxylamine is thought to occur in two, two-electron steps, with the tyrosine attached to P460 allowing it to transiently accept two electrons [5-6]. Trimerisation is necessary for catalysis, allowing a tyrosine residue from one subunit to cross-link to P460 from a neighbouring subunit, and providing a hydrophobic environment for the haem groups where stable electron transfer can occur. The nitrite ion, which has the chemical formula NO_2^-, is a symmetric anion with equal N-O bond lengths and an O-N-O bond angle of approximately 120° [7-8]. Upon protonation, the unstable weak acid nitrous acid is produced. Nitrite can be oxidized or reduced, with the product somewhat dependent on the oxidizing/reducing agent and its strength. The nitrite ion is an ambidentate ligand, and is known to bond to metal centers in at least five different ways [9-11]. Nitrite is also important in biochemistry as a source of the potent vasodilator nitric oxide. In organic chemistry the NO_2 group is present in nitrous acid esters and nitro compounds. Nitrites are also used in the food production industry for curing meat [12]. A biosensor is an analytical device comprising two elements in spatial proximity: A biological recognition element able to interact specifically with a target and a transducer that is able to convert the recognition event into a measurable signal; in other word a biosensor is an analytical device which converts a biological response into an electrical signal [13-16]. The term 'biosensor' is often used to cover sensor devices used in order to determine the concentration of substances and other parameters of biological interest even where they do not utilise a biological system directly. The biological response of the biosensor is determined by the biocatalytic membrane which accomplishes the conversion of reactant to product [17-19]. Immobilised enzymes possess a number of advantageous features which makes them particularly applicable for use in such systems [20-21]. Many enzymes are intrinsically stabilised by the immobilisation process, but even where this does not occur there is usually considerable apparent stabilisation. It is normal to use an excess of the enzyme within the immobilised sensor system. One of the most important functions of nanoparticles is catalysis, especially with noble metal nanoparticles, which have high catalytic activity for many chemical reactions [22-25]. Nanoparticle based biosensors have the distinct advantage over macroscopic biosensors in that they can penetrate into environments normal sensors cannot reach and also an ensemble of nanoparticle biosensors can be located throughout an entire sample greater sensitivity and shorter response times are possible[26-29]. In this work, we designed a biosensor based on Hydroxylamine oxidase and modified electrode with ZnO nanoparticles. This biosensor introduced new and cheap way for detection of Nitrite (NO_2) and hydroxylamine.

2. EXPERIMENTAL

2.1. Materials

Hydroxylamine, Hydroxylamine oxidase and Nitrite were purchased from sigma-aldrich and other chemicals used were purchased from Merck Company. Phosphate buffer solutions (PBS, 0.2M) with various pH values were prepared by mixing stock standard solutions of Na_2HPO_4 and NaH_2PO_4 and adjusting the pH with H_3PO_4 or NaOH. All other chemicals were of analytical grade and all the solutions were prepared with doubly distilled water.

2.2. Apparatus

Cyclic voltammetric (CV) experiments were performed with a model EA-201 Electro Analyzer (chemilink systems), equipped with a personal computer was used for electrochemical measurement and treating of data. A conventional three electrode cell was employed throughout the experiments, with bare or Zno nanoparticles modified carbon paste electrode (4.0 mm diameter) as a working electrode, an Ag/AgCl as a reference electrode and a platinum electrode as a counter electrode. Samples were measured and recorded using a TU-1901 double-beam UV-visible spectrophotometer and were dispersed in toluene solution. The phase characterization was performed by means of X-ray diffraction (XRD) using a D/Max-RA diffractometer with CuKα radiation. The experimental solutions were de-aerated using highly pure nitrogen for 30 min. and a nitrogen atmosphere was kept over the solutions during the measurements. The morphologies and particle sizes of the samples were characterized by scanning electron microscopy (SEM) images were obtained with a ZIESS EM 902A scanning electron microscope. All the electrochemical measurements were carried out in 0.1 M PBS, pH 7.0 at 25 ± 1 ^{o}C.

2.3. Synthesis of ZnO Nanoparticles

To prepare of ZnO NPs, in a typical experiment, a 0.45 M aqueous solution of zinc nitrate (Zn $(NO_3)_2.4H_2O$) and 0.9 M aqueous solution of sodium hydroxide (NaOH) were prepared in distilled water. Then, the beaker containing NaOH solution was heated at the temperature of about 55 ºC. The Zn $(NO_3)_2$ solutions were added drop wise (slowly for 1h) to the above heated solution under high speed stirring. The beaker was sealed at this condition for 2 h. The precipitated ZnO NPs was cleaned with deionized water and ethanol then dried in air atmosphere at about 60 ºC.

2.4. Preparation of Zno nanoparticles modified carbon paste electrode

The Zno nanoparticles modified carbon paste electrode was prepared by hand mixing of carbon powder, binder and 10 mg Zno nanoparticle with silicon oil in an agate mortar to produce a homogenous carbon paste. Other steps of produced modified carbon paste electrode were similar to preparation of bare carbon paste electrode. A conventional three electrode cell was employed

throughout the experiments, with bare or ZnO nanoparticles modified carbon paste electrode (4.0 mm diameter) as a working electrode, an Ag/AgCl as a reference electrode and a platinum electrode as a counter electrode.

2.5. Preparation of HAO-Zno nanoparticles modified carbon paste electrode

The modified electrode that produced in previous section was used for production of HAO-Zno nanoparticles modified carbon paste electrode. In this section, the HAO was immobilized by dropping 5 µl of 10 mg/ml of the enzyme solution onto the Zno nanoparticles modified carbon paste electrode and dried for about 30 min. at room temperature. The electrode was then gently washed with de-ionized double distilled water and put at 4 ºC when not in use.

3. RESULTS AND DISCUSSION

3.1. Scanning electron microscopy (SEM) study of Zno nanoparticles

As it is well known, the properties of a broad range of materials and the performance of a large variety of devices depend strongly on their surface characteristics [30-33]. For instance, the surface of a biomaterial/biomedical device meets the physiological environment, immediately after it is placed in the body or bloodstream and the initial contact regulates its subsequent performance [34]. The average diameter of the synthezd Zno nanoparticles is about 34 nm, and has a very narrow particle distribution. This statement illustrated in figure 1. Fig. 1 Show a SEM picture of the Zno nanoparticles. As the size of nanoparticles decreased, the ratio of surface-to-volume increased. This feature represents the significant role of nanoparticles in immobilization processes. Based on SEM results, the scale bars in Fig. 1a and 1b represent 500 nm and 200 nm, respectively.

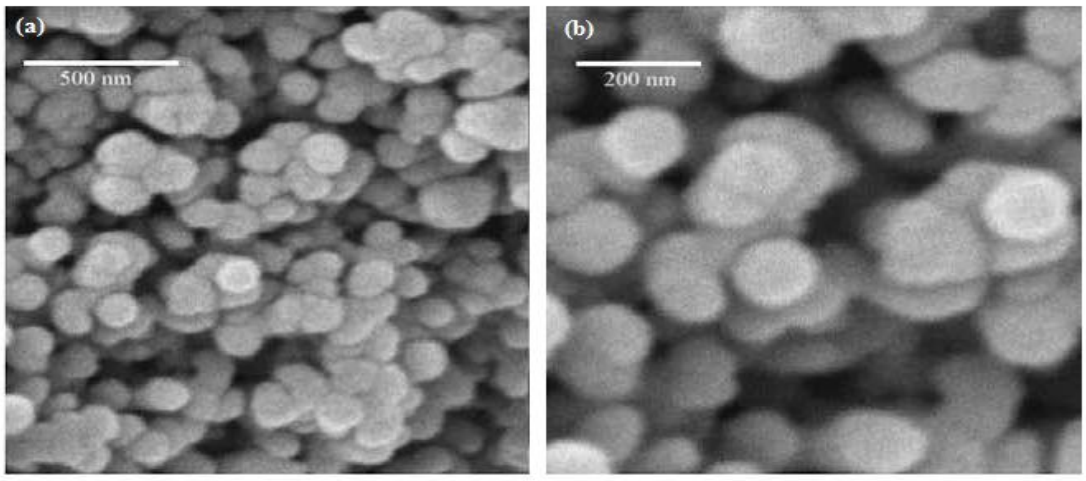

Figure 1. SEM image of the Zno nanoparticles; (a) the scale bar is 500 nm and (b) the scale bar is 200 nm

3.2. UV–visible absorption spectra of Zno nanoparticles

The UV–visible absorption spectra of Zno nanoparticles are shown in Figure 2. The absorption band of the Zno nanoparticles exhibits increase due to the quantum confinement in sample compared to bulk Zno particles. This optical phenomenon indicated that these nanoparticles showed the quantum size effect [35-36].

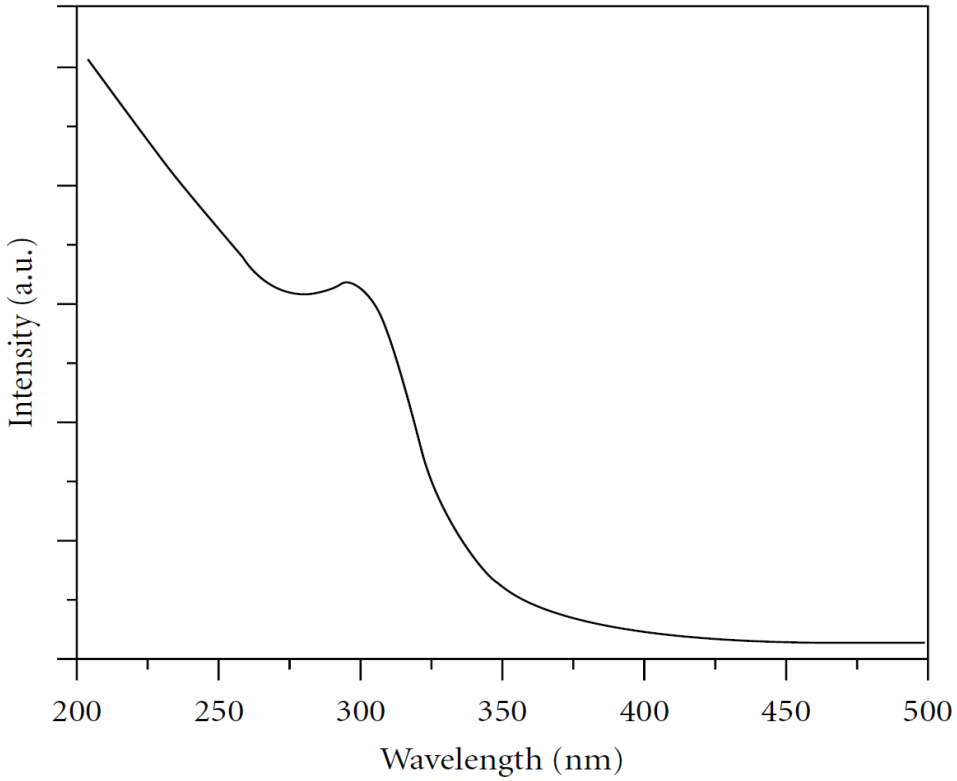

Figure 2. UV-VIS spectra for Zno nanoparticles; the shift occurred in ~ 300 nm wavelength

3.3. X-Ray diffraction of Zno nanoparticles

The x-ray diffraction data were recorded by using Cu Kα radiation (1.5406 A^o). The intensity data were collected over a 2θ range of 20-80^o. The average grain size of the samples was estimated with the help of Scherrer equation using the diffraction intensity of (101) peak. x-ray diffraction studies confirmed that the synthesized materials were ZnO with wurtzite phase and all the diffraction peaks agreed with the reported JCPDS data and no characteristic peaks were observed other than ZnO. The mean grain size (D) of the particles was determined from the XRD line broadening measurement using Scherrer equation [37]:

$$D=0.89\lambda / (\beta Cos\theta) \quad (1)$$

Where λ is the wavelength (Cu Kα), β is the full width at the half- maximum (FWHM) of the ZnO (101) line and θ is the diffraction angle. A definite line broadening of the diffraction peaks is an indication that the synthesized materials are in nanometer range [38]. The lattice parameters calculated were also in agreement with the reported values. The reaction temperature greatly influences the particle morphology of as-prepared ZnO powders. Figure 3 (a &b) shows the XRD patterns of ZnO

nanoparticles. The size of particles estimated using the relative peak intensity was found to be 34 nm for ZnO NPs, and increase in the sharpness of XRD peaks indicated that particles were crystalline in nature.

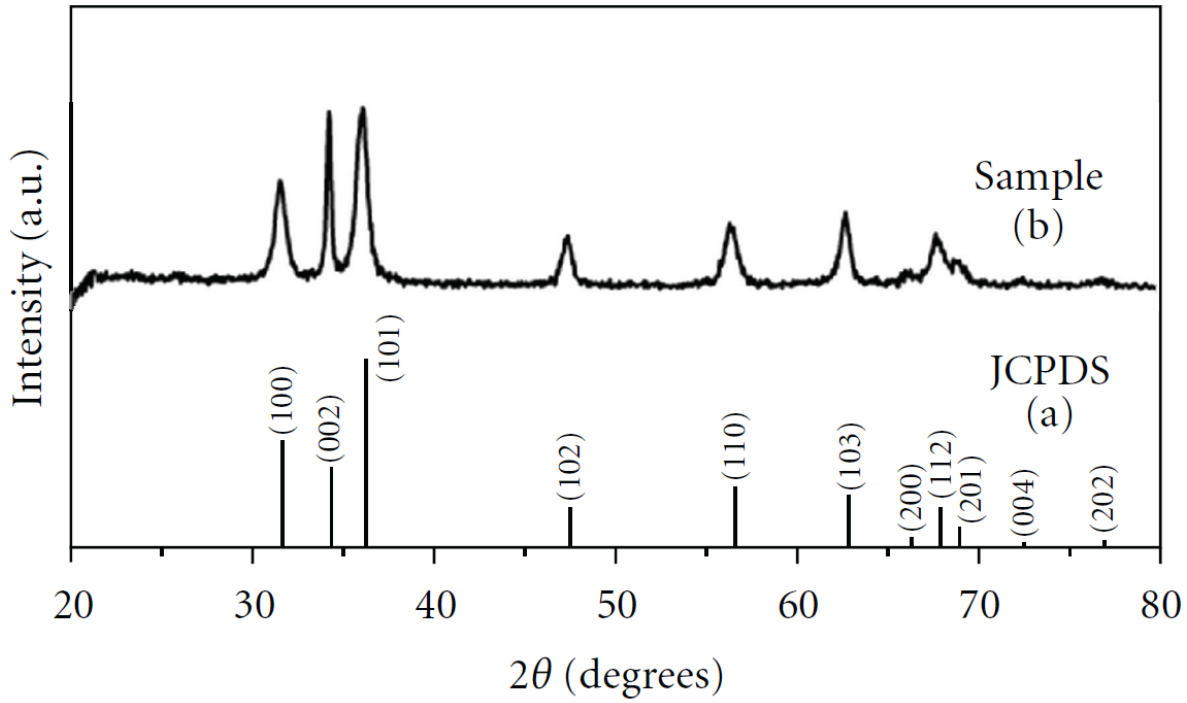

Figure 3. X-Ray diffraction of Zno nanoparticles; (a) about Joint Committee for Powder Diffraction (JCPDS) and (b) about sample

3.4. Direct electrochemistry of HAO / Zno nanoparticles /carbon paste electrode

The integrity of the immobilized myoglobin construction and its ability to exchange electrons with the nanometer- scale Zno particles surfaces were assessed by voltammetry. A macroscopic electrode was required to attain a large enough Hydroxylamine oxidase sample to yield detectable direct oxidation and reduction currents. The comparative CVs for the Zno NPs/CPE and HAO / Zno NPs/ CPE electrodes in 0.1 M PBS (pH 7.0) was obtained. These voltammograms are demonstrated in Figure 4 (a,b). From this Figure, it was noticed that there were no voltammetric response on Zno NPs/carbon paste electrode (Fig. 4a), which, Fig. 4b depicts a well-defined pair of oxidation–reduction (redox) peaks, observed on the HAO / Zno NPs/ carbon paste electrode at 100 mv/s scan rate value. The HAO / Zno NPs/ carbon paste electrode presented the reductive peak potential at +155 mV and the corresponding oxidative peak potential at +205 mV (at 100 mV s^{-1}), illustrating the adsorbed Hydroxylamine oxidase on the nanometer-scale zinc oxide particles surfaces. The difference of anodic and cathodic peak potential values was ΔE = 50 mV. These redox peaks were attributed to the redox reaction of the Hydroxylamine oxidase electroactive center. The formal potential (E^0) for the Hydroxylamine oxidase redox reaction on the HAO / Zno NPs/ carbon paste electrode was 180 mV with respect to the reference (Ag/ Agcl) electrode. The collected voltammograms in Figure 5 (a)

substantiated this statement that the nanometer-scale zinc oxide particles could play a key role in the observation of the Hydroxylamine oxidase CV response.

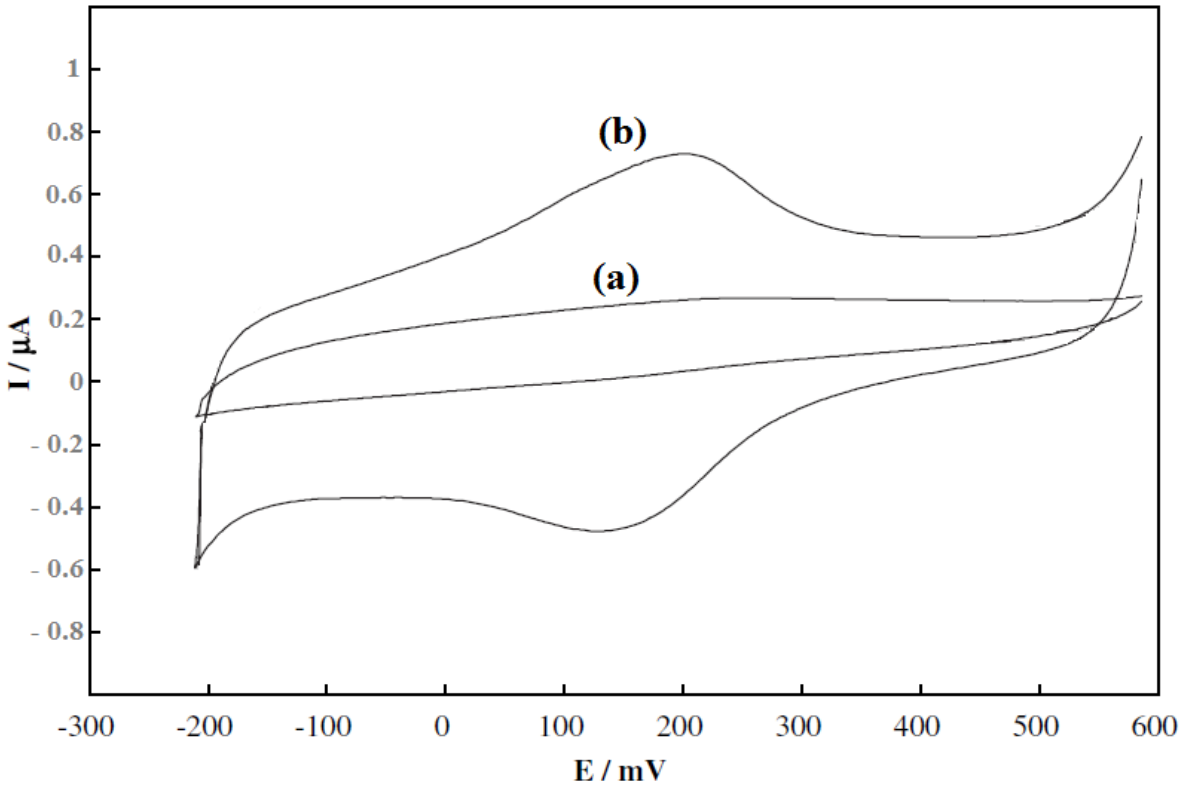

Figure 4. Cyclic voltammograms, using (a) the ZnoNPs/CPE in 0.1 M phosphate buffer solution (PBS) and (b) HAO / Zno NPs/ CPE in 0.1 M phosphate buffer (scan rate: 100 mV/s).

On the grounds that the surface-to-volume ratio increases with the size decrease and because of the fact that the enzyme size is comparable with the nanometer-scale building blocks, these nanoparticles displayed a great effect on the electron exchange assistance between Hydroxylamine oxidase and carbon paste electrode. To further investigate the Hydroxylamine oxidase characteristics at the HAO / Zno NPs/ CPE electrode, the effect of scan rates on the Hydroxylamine oxidase voltammetric behavior was studied in detail. The baseline subtraction procedure for the cyclic voltammograms was obtained in accordance with the method reported by Bard and Faulkner [39]. The scan rate (ν) and the square root scan rate ($\nu^{1/2}$) dependence of the heights and potentials of the peaks are plotted in Figure 5 (b) and 5 (c). It can be seen that the redox peak currents increased linearly with the scan rate, the correlation coefficient was 0.9959 (ipc = -0.0062ν + 0.0958) and 0.9972 (ipa = +0.0062ν + 0.5897), respectively. This phenomenon suggested that the redox process was an adsorption-controlled and the immobilized Hydroxylamine oxidase was stable. It can be seen that the redox peak currents increased more linearly with the ν in comparison to that of $\nu^{1/2}$.

However, there is clearly a systematic deviation from linearity in this data, i.e. low scan rates are always on one side of the line and the high scan rate points are on the other. The anodic and

cathodic peak potentials are linearly dependent on the logarithm of the scan rates (ν) when ν > 1.0 V s^{-1}, which was in agreement with the Laviron theory, with slopes of -2.3RT/αnF and 2.3RT/ (1 -α) nF for the cathodic and the anodic peak, respectively [40]. So, the charge-transfer coefficient (α) was estimated as 0.59. Furthermore, the heterogeneous electron transfer rate constant (ks) was estimated according to the following equation [41]:

$$[\log ks = \alpha \log(1-\alpha) + (1-\alpha)\log\alpha - \log\frac{RT}{nF\nu} - \frac{\alpha(1-\alpha)nF\Delta EP}{2.3\,RT}] \quad (2)$$

Here, n is the number of transferred electrons at the rate of determining reaction and R, T and F symbols having their conventional meanings.

R, F and T are gas constant, Faraday constant and absolute temperature, respectively, all having definite values:

R = 8.314 J mol-1 K-1 , F = 96493 C/mol , T = 298 K

ΔE_p is the peak potential separation, giving an average heterogeneous transfer rate constant (ks) value of 1.33 s^{-1}.

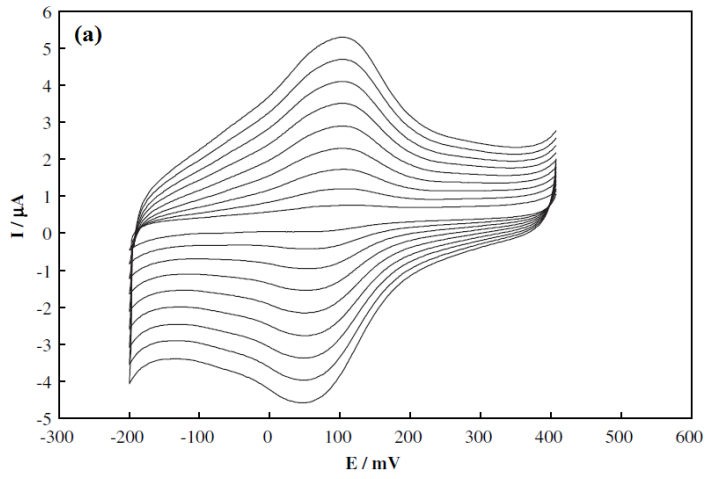

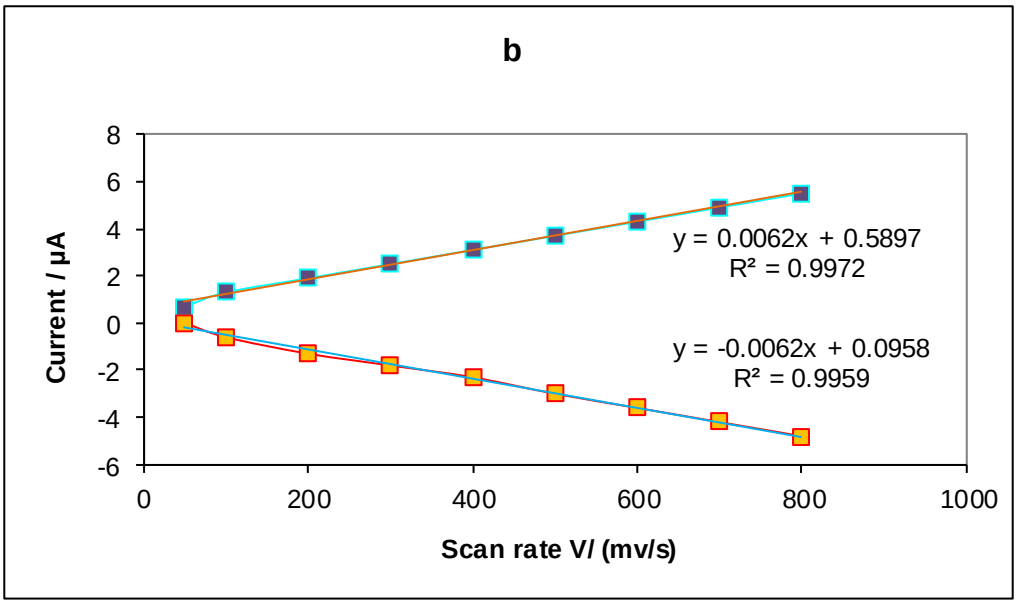

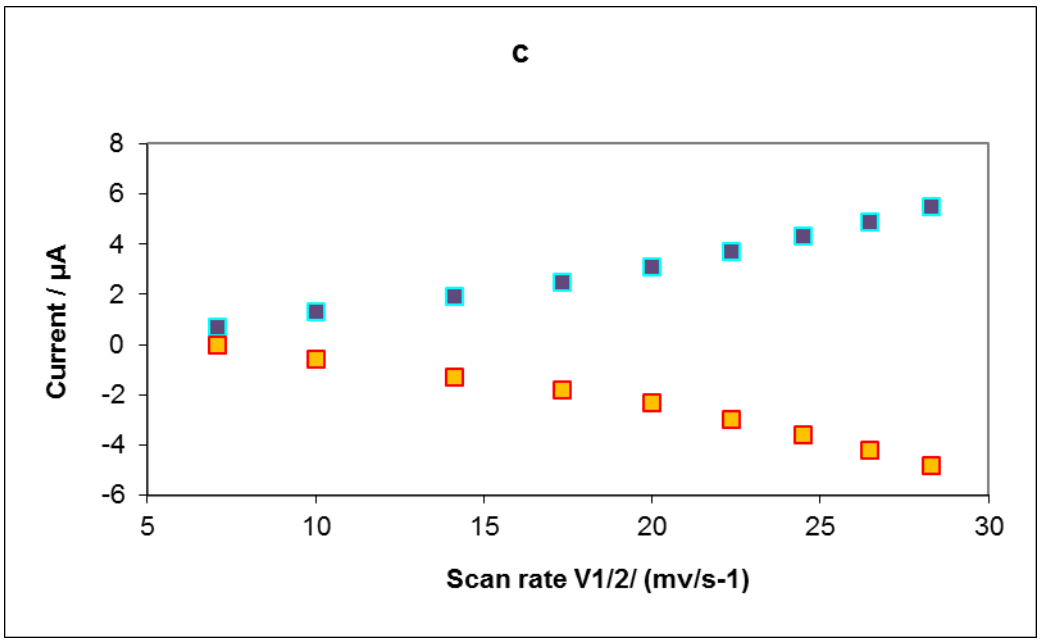

Figure 5. (a) CVs of HAO / Zno NPs/ CPE electrode in PBS at various scan rates, from inner to outer; 50, 100, 200, 300, 400, 500, 600, 700 and 800 mV s^{-1}, the relationship between the peak currents (ipa, ipc) vs., (b) the sweep rates and (c) the square root of sweep rates.

3.5. Electrocatalysis of HAO / Zno NPs/ CPE to detect NO_2^- and NH_2OH

Upon addition of NO_2^- to 0.1M pH 7.0 PBS, the cyclic voltammogram of the HAO / Zno NPs/CPE electrode for the direct electron transfer of Hydroxylamine oxidase changed dramatically with an increase of oxidation peak current and a decrease of reduction peak current (Fig. 6 a), while the change of cyclic voltammogram of bare or Zno Nps/ CPE was negligible (not shown), displaying an obvious electrocatalytic behavior of the Hydroxylamine oxidase to the reduction of NO_2^-. The decreases of the reductive peak current were together with the increases of the oxidative of HAO / Zno NPs/CPE. The electro-catalytic process could be expressed as follows:

$$Fe_{II}\text{-}HNO + NO + H^+ \rightarrow Fe_{III} + N_2O + H_2O \quad (3)$$

$$Fe_{II} + NO \leftrightarrow Fe_{II}\text{-}NO \quad (4)$$

$$Fe_{II}\text{-}NO + e^- + H^+ \leftrightarrow Fe_{II}\text{-}HNO \quad (5)$$

$$Fe_{II}\text{-}HNO + 2H^+ + 2e^- \rightarrow Fe_{II} + H_2NOH \quad (6)$$

In enzymology, a hydroxylamine oxidase (EC 1.7.3.4) is an enzyme that catalyzes the chemical reaction:

$$\text{Hydroxylamine} + O_2 \leftrightarrow \text{nitrite} + H_2O \quad (7)$$

Thus, the two substrates of this enzyme are hydroxylamine and O_2, whereas its two products are nitrite and H_2O [42]. The heme pairs function as redox centers in electron transfer Mid-point potentials have not been assigned to specific hemes [43-44]. This enzyme belongs to the family of oxidoreductases, specifically those acting on other nitrogenous compounds as donors with oxygen as acceptor [45].

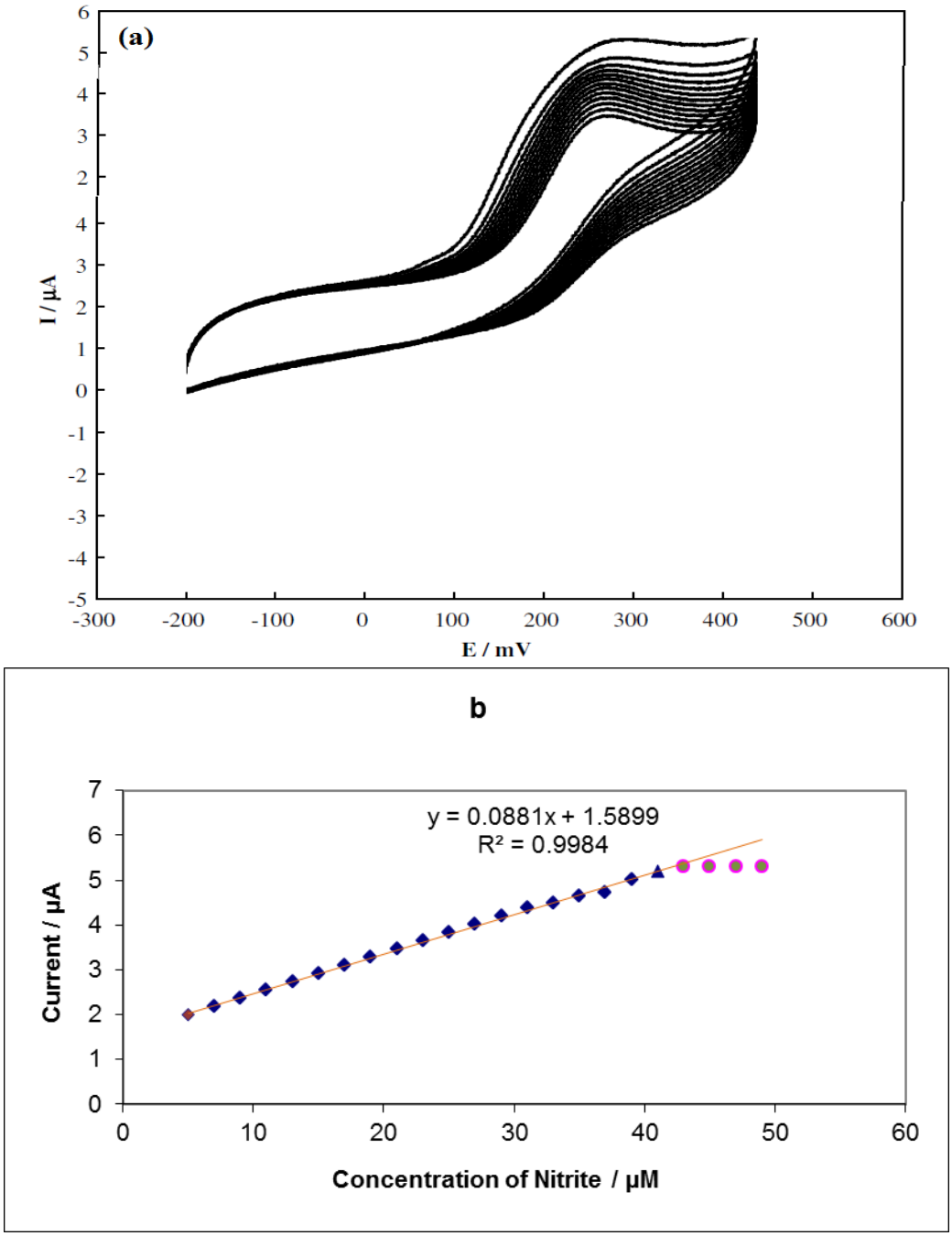

Figure 5. (a) Cyclic voltammograms obtained at an HAO / Zno NPs/CPE electrode in 0.1M phosphate buffer solution (pH 7.0) for different concentrations of and (b) the relationship between anodic peak current of Hydroxylamine oxidase and different concentrations of NO_2^- (scan rate: 100 mVs $^{-1}$).

For each turnover of hydroxylamine oxidase one molecule of hydroxylamine is oxidized to nitrite, with the associated four electrons being transferred to the Quinone pool. Half of the resultant quinoas transfer electrons to the ammonia mono-oxygenase so that one molecule of hydroxylamine is generated from each molecule of ammonia [46-47]. The calibration curve (Figure 6 b) shows the linear dependence of the anodic peak current on the NO_2^- concentration in the range of 5 to 43 μM. In Figure 6 (b), at higher concentration of NO_2^- , the anodic peak current decreased and remains constant. Upon addition of an aliquot of NO_2^- to the buffer solution, the oxidation current increased steeply to reach a stable value (Fig 6 b). This implies electrocatalytic property of electrode. Thus, this experiment has introduced a new biosensor for the sensitive determination of NO_2^- in solution and also determination of Hydroxylamine at surface of working electrode (here CPE) ; Figure 6. (a) Cyclic voltammograms obtained at an HAO / Zno NPs/CPE in 0.1M phosphate buffer solution (pH 7.0) for different concentrations of and Figure 6. (b) Show the relationship between anodic peak current of Hydroxylamine oxidase and different concentrations of NO_2^- (scan rate: 100 mVs^{-1}).

3.6. Stability of biosensor

The stability of HAO / Zno NPs/CPE electrode biosensor has been checked by carrying out experiments at the regular interval of a week and it has been found that HAO / Zno NPs/CPE electrode based optical biosensor retains its 91% activity after 30 days. The loss in the activity of biosensor is not due to the denaturation of Hydroxylamine oxidase but it is due to the poor adhesion of zinc oxide Nanoparticles on the carbon paste electrode. If we able to increase purity percentage of zinc oxide nanoparticles, we hope adhesion of these nanoparticles will be improved. For a result, interface materials have not high effect on operation of this biosensor.

4. CONCLUSION

Today, the design biosensors, Nano-science, electrochemistry and biophysics are being used. An important purpose of designed biosensors is the exact detect of chemical composition in ranges of very small. In this study we introduced a new way for detect NO_2^- and (NH_2OH). Our biosensor showed good response and Stability against interface materials and other electrochemical challenge.

References

1. Averill, B. A., *Chem. Rev*. 96 (1996) 2951.
2. Janssen, L. J. J.; Pieterse, M. M. J.; Barendrecht, E., *Electrochim. Acta*, 22 (1977) 27.
3. de Vooys, A. C. A.; Koper, M. T. M.; van Santen, R. A.; van Veen, J. A. R., *J. Catal*. 202 (2001) 387.
4. de Vooys, A. C. A.; Koper, M. T. M.; van Santen, R. A.; van Veen, J. A. R., *Electrochim. Acta*, 46 (2001) 923-930.
5. Wasser, I. M.; de Vries, S.; Moeenne-Loccoz, P.; Schroeder, I.; Karlin, K. D., *Chem. Rev*. 102 (2002) 1201.

6. Otsuka, K.; Sawada, H.; Yamanaka, I., *J. Electrochem. Soc*. 143 (1996) 3491.
7. Kudo, T.; Takaya, N.; Park, S.-Y.; Shiro, Y.; Shoun, H., *J. Biol. Chem*. 276 (2001) 5020.
8. Einsle, O.; Messerschmidt, A.; Huber, R.; Kroneck, P. M. H.; Neese, F., *J. Am. Chem. Soc*. 124 (2002) 11737.
9. J. J. Lingane, Electroanalytical chemistry, Second ed., *Wiley-Interscience, New York*, 1958.
10. C. Ren, Y. Song, Z. Li, G. Zhu, *Anal. Bioanal. Chem*., 381 (2005) 1179.
11. A. Salimi, E. Sharifi, A. Noorbakhsh, S. Soltanian, *Biophys. Chem*. 125 (2007) 540.
12. D. Britz, *J. Electroanal. Chem*. 88 (1978) 309.
13. Sanford, C.L.; Mantooth, B.A.; Jones, B.T. *J. Chem. Educ*., 78 (2001) 1221.
14. C.C. Moser, C.C. Page, R. Farid, P.L. *J Bioenerg Biomembr*, 27 (1995) 263.
15. M. Negahdary, M. Torkamani-Noughabi, E. Rezaei, *Advances in Environmental Biology*. 6 (2012) 1095.
16. S. Rezaei-Zarchi, M. Negahdary, *Advances in Environmental Biology*, 5 (2011) 3241.
17. M. Negahdary, C. Mazaheri, S. Rad, M. Hadi, R.Malekzadeh, *International Journal of Analytical Chemistry*, 2012(2012) 1.
18. R. Feynman, There's plenty of room at the bottom. In: *Miniaturization (ed. H.D. Gilbert), New York*, 1961.
19. R. Kurzweil, The Singularity is Near: When humans transcend biology, New York: *Viking Press*, 2005.
20. J.J. Ramsden, Nanotechnology Perceptions, 1 (2005) 3.
21. W. Banzhaf et al., *Nature Reviews Genetics*. 7 (2006) 729.
22. C. Hierold, *J. Micromech. Microengng*. 14 (2004) S1.
23. Jeremy Ramsden, Essentials of Nanotechnology, *Ventus Publishing ApS*. 2009.
24. J. J. Lingane, Electroanalytical chemistry, Second ed., *Wiley-Interscience, New York*, 1958.
25. F. Scheller, F. Schubert, Biosensors, Elsevier, 1992.
26. Xie, X., Subiman, A.A., Guilbault, G.G. and Yang, Z. *Anal.Chim. Acta* 266 (1992) 325.
27. D. P. Hildebrand, H. Tang, Y. Luo, C. L. Hunter, M. Smith, G. D. Brayer, A. G. Mauk, *J. Am. Chem. Soc*. 118 (1996) 12909.
28. Rizzuto *et al*. *J. Biol. Chem*. 264 (1989) 10595.
29. J. F. Rusling, A.-E. F. Nassar, *J. Am. Chem. Soc*. 115 (1993) 11891.
30. A.-E. F. Nassar, J. M. Bobbitt, J. D. Struart, J. F. Rusling, *J. Am. Chem. Soc*. 117 (1995) 10986.
31. Gholamreza Mohseni, Masoud Negahdary, *Int. J. Electrochem. Sci*., 7 (2012) 7033.
32. M. F. Perutz, M. G. Rossmann, A. F. Cullis, H. Muirhead, *Nature*, 185 (1960) 416.
33. M. Brunori and Q. H. Gibson., *EMBO Rep*. 2 (2001) 676.
34. T. Kuo, M.H. Huang, *J. Phys. Chem B*. 110 (2006) 13717.
35. M. Negahdary, S. Rad, M. Torkamani Noughabi, *Advanced Studies in Biology*, 4 (2012) 103.
36. V. Drits, J. Środoń and D. D. *Reappraisal of the Kubler Index and the Scherrer Equation Clays and Clay Minerals*. 45 (1997) 461.
37. H. Fan, L. Yang, W. Hua et al., *Nanotechnology*, 15 (2004) 37.
38. Masoud Negahdary, Saeed Rezaei-Zarchi, *ISRN Biophysics*. 2012(2012) 1.
39. D. R. Crow, Principles and applications of electrochemistry, 3rd edn, *Chapman and Hall, London*, 1988.
40. E. Laviron, *J. Electroanal. Chem*., 100 (1979) 263.
41. S. Banapour, M. Mazdapour, Z. Dinpazhooh, F. Salahi, M. Torkamani Noughabi, M. Negahdary, A. Asrari, F. Ghanami, *Advanced Studies in Biology*, 4 (2012) 231.
42. M. Negahdary, S. Rad, M. Torkamani Noughabi, *Advanced Studies in Biology*, 4 (2012) 103.
43. Yoshida, T. & Alexander, M. Can. *J. Microbiol*. 10 (1964) 923.
44. Ritchie, G. A. F. & Nicholas, D. J. D. *Biochem. J.* 126 (1972) 1181.
45. Terry, K. and Hooper, A. B. *Biochemistry.* 20 (1981) 7026.
46. Arciero, D. M. and Hooper, A. B. *J. Biol. Chem*. 268 (1993) 14645.

47. Wood, P. M. (1986) in Nitri®cation (Prosser, J., ed.) (Spec. Publ. Soc. Gen. Microbiol. 20), pp. 63-78, IRL Press, Oxford